Available online at www.sciencedirect.com
ScienceDirect
Dyes and Pigments 74 (2007) 169–175
DYES and PIGMENTS
www.elsevier.com/locate/dyepig

Properties of novel perylene-3,4:9,10-tetracarboxidiimide-centred dendrimers and their application as emitters in organic electroluminescence devices

Masaki Matsui [a,*], Mingxing Wang [a], Kazumasa Funabiki [a], Yoshio Hayakawa [b], Toru Kitaguchi [c]

[a] *Department of Materials Science and Technology, Faculty of Engineering, Gifu University, Yanagido, Gifu 501-1193, Japan*
[b] *National Institute of Advanced Industrial Science and Technology, 2266-98 Anagahora, Sidami, Moriyama, Nagoya 463-8560, Japan*
[c] *Daicel Chemical Industries, Ltd. 1239 Shinzaike, Aboshi-ku, Himezi, Hyogo 671-1283, Japan*

Received 21 January 2006; received in revised form 24 January 2006; accepted 26 January 2006
Available online 20 March 2006

Abstract

The UV−vis absorption and fluorescence spectra, solubility, and application as emitters in single-layer EL devices of novel perylene-3,4:9,10-tetracarboxidiimide-centred dendrimers (**G_n-Perys**) were examined. **G_n-Perys** showed absorption maxima (λ_{max}) at 459, 491, and 529 nm in chloroform. The emission maxima (λ_{em}) were observed at 537, 576, and 621 nm. The fluorescence intensities of **G_1-**, **G_2-**, and **G_3-Perys** were ca. one-twentieth compared with that of **G_0-Pery**. However, the concentration-quenching of **G_n-Perys** ($n = 1, 2, 3$) was improved. The solubility of **G_n-Perys** increased at higher generation. The electroluminescence (EL) maxima of **G_n-Perys** in single-layer EL devices containing PVK and PBD as host materials were observed at around 430 and 600 nm, there being white emission. No remarkable difference in the EL characteristics was observed among **G_n-Perys**.

Keywords: Perylenecarboxidiimide; Dendrimer; Fluorescence spectra; Solubility; UV−vis absorption spectra; Emitter

1. Introduction

Much attention has been paid to dendrimers due to their unique properties. Azobenzene-centred dendrimer displays *cis*−*trans* isomerization by irradiating infrared light [1] while rhodamine-centred dendrimers have been reported to show high-fluorescence efficiency [2]. Silicon phthalocyanines with *axial* dendritic substituents have been reported to have a glass transition in the range of 110−139 °C [3]. Meanwhile, **Perys** are interesting advanced materials which have potential application as charge-generation materials in organic photoconductors [4], and sensitizers for dye-sensitized solar cells [5]. The application of polyfluorene attached to perylene dyes [6] and perylenetetracarboxidiimide having polyphenylene dendrons [7] as light-emitting materials has been also reported. This paper concerns the basic properties such as UV−vis absorption and fluorescence spectra and solubility of **G_n-Perys** and their applications as emitters in single-layer EL devices.

2. Experimental

2.1. Instruments

Melting points were measured on a Yanagimoto MP-52 micro-melting-point apparatus. High-performance liquid chromatography was performed using a Jasco Gulliver series and NMR spectra were obtained on a Varian Inova 500 spectrometer. EIMS spectra were measured using a Jeol MStation 700

* Corresponding author. Tel.: +81 58 293 2601; fax: +81 58 230 1893.
E-mail address: matsui@apchem.gifu-u.ac.jp (M. Matsui).

0143-7208/$ - see front matter © 2006 Elsevier Ltd. All rights reserved.
doi:10.1016/j.dyepig.2006.01.031

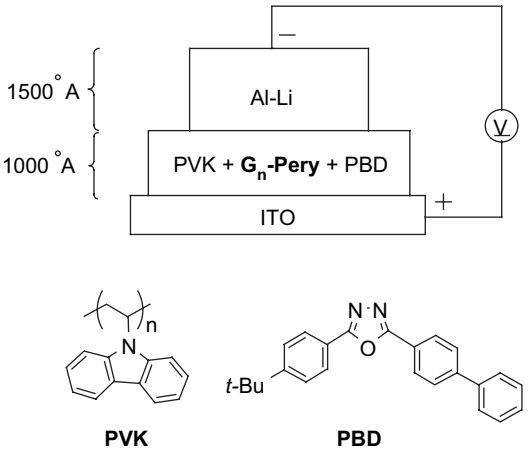

Fig. 1. EL device and chemical structures of PVK and PBD.

spectrometer and UV–vis absorption and fluorescence spectra were obtained using a Hitachi U-3500 and F4500 spectrophotometers, respectively. Elemental analysis was performed using a Yanaco MT-6 CHN corder.

2.2. Materials

3,4:9,10-Perylenetetracarboxylic dianhydride was purchased from Tokyo Kasei Co., Ltd. 3,5-Di-*tert*-butylbenzyl bromides **G_0-Br**, **G_1-Br**, **G_2-Br**, and **G_3-Br** and **G_0-NH_2** were synthesized as described in the literature [8].

2.3. Synthesis of phthalimides (***G_n-NP***)

A suspension of **G_n-Br** (1.5 mmol) and potassium phthalimide (1.8 mmol) in dry DMF (10 ml) was heated at 70–75 °C for 5 h. After the reaction was complete, the reaction mixture was cooled to room temperature and water (20 ml) was added. The resulting yellow oil was extracted with dichloromethane (15 ml × 2). The organic layer was dried over anhydrous sodium sulfate, filtered, and evaporated to provide a yellow syrup, which was solidified by adding methanol.

2.3.1. N-[3,5-Di(tert-butyl)benzyl]phthalimide (***G_0-NP***)

Yield 80%; mp 141–143 °C; ^{1}H NMR ($CDCl_3$) $\delta = 1.31$ (s, 18H), 4.85 (s, 2H), 7.34–7.36 (m, 3H), 7.68–7.70 (m, 2H), 7.83–7.85 (m, 2H); EIMS (70 eV) *m/z* (rel intensity) 349 (M^+, 25), 334 (100), 292 (17), 160 (88), 131 (27), 77 (16), 57 (67).

2.3.2. N-{3,5-Bis[3,5-di(tert-butyl)benzyloxy]benzyl} phthalimide (***G_1-NP***)

Yield 94%; mp 196–198 °C; ^{1}H NMR ($CDCl_3$) $\delta = 1.33$ (s, 36H), 4.81(s, 2H), 4.96 (s, 4H), 6.59 (t, $J = 2.3$ Hz, 1H), 6.71 (d, $J = 2.3$ Hz, 2H), 7.25 (d, $J = 1.8$ Hz, 4H), 7.39 (t, $J = 1.8$ Hz, 2H), 7.70–7.72 (m, 2H), 7.85–7.86 (m, 2H); EIMS (70 eV) *m/z* (rel intensity) 470 (M^+-(3,5-di-*tert*-butylbenzyl) + H, 24), 203 (100), 57 (32).

2.3.3. N-(3,5-Bis{3,5-bis[3,5-di(tert-butyl)benzyloxy] benzyloxy}benzyl)phthalimide (***G_2-NP***)

Yield 90%; mp 85–87 °C; ^{1}H NMR ($CDCl_3$) $\delta = 1.33$ (s, 72H), 4.79 (s, 2H), 4.96 (s, 4H), 4.99 (s, 8H), 6.55 (t, $J = 2.1$ Hz, 1H), 6.62 (t, $J = 2.1$ Hz, 2H), 6.68 (d, $J = 2.1$ Hz, 2H), 6.71 (d, $J = 2.1$ Hz, 4H), 7.27 (d, $J = 1.8$ Hz, 8H), 7.40 (t, $J = 1.8$ Hz, 4H), 7.67–7.69 (m, 2H), 7.81–7.83 (m, 2H).

2.3.4. N-[3,5-Bis(3,5-bis{3,5-bis[3,5-di(tert-butyl) benzyloxy]benzyloxy}benzyloxy)-benzyl]phthalimide (***G_3-NP***)

Yield 75%; mp 91–93 °C; ^{1}H NMR ($CDCl_3$) $\delta = 1.31$ (s, 144H), 4.77 (br, 2H), 5.00 (s, 28H), 6.55–6.73 (m, 21H), 7.27 (d, $J = 1.7$ Hz, 16H), 7.39 (t, $J = 1.7$ Hz, 8H), 7.61–7.63 (m, 2H), 7.79–7.81 (m, 2H).

2.4. Synthesis of ***G_n-NH_2***

An ethanol suspension (10 ml) of **G_n-NP** (1 mmol) and hydrazine monohydrate (0.5 ml) was refluxed for 20 min at the end of which, a white gelatinous precipitate was formed. After cooling the mixture to room temperature, 20% aqueous potassium hydroxide (50 ml) was added and the ensuing product was extracted with ether (50 ml × 3). The extract was dried over anhydrous sodium sulfate; the crude product was purified by column chromatography (SiO_2, dichloromethane).

2.4.1. 3,5-Bis[3,5-di(tert-butyl)benzyloxy]benzylamine (***G_1-NH_2***)

Yield 80%; mp 81–83 °C; ^{1}H NMR ($CDCl_3$) $\delta = 1.34$ (s, 36H), 3.83 (s, 2H), 5.01 (s, 4H), 6.58 (t, $J = 2.3$ Hz, 1H), 6.61 (d, $J = 2.3$ Hz, 2H), 7.28 (d, $J = 1.8$ Hz, 4H), 7.41 (t, $J = 1.8$ Hz, 2H).

2.4.2. 3,5-Bis{3,5-bis[3,5-di(tert-butyl)benzyloxy] benzyloxy}benzylamine (***G_2-NH_2***)

Yield 80%; mp 72–74 °C; ^{1}H NMR ($CDCl_3$) $\delta = 1.33$ (s, 72H), 2.18 (s, 2H), 3.82 (s, 2H), 5.00 (s, 12H), 6.54 (t, $J = 2.5$ Hz, 1H), 6.58 (d, $J = 2.5$ Hz, 2H), 6.65 (t, $J = 1.9$ Hz, 2H), 6.73 (d, $J = 1.9$ Hz, 4H), 7.28 (d, $J = 1.8$ Hz, 8H), 7.41 (t, $J = 1.8$ Hz, 4H).

2.4.3. 3,5-Bis(3,5-bis{3,5-bis[3,5-di(tert-butyl)benzyloxy] benzyloxy}benzyloxy)-benzylamine (***G_3-NH_2***)

Yield 72%; mp 85–87 °C; ^{1}H NMR ($CDCl_3$) $\delta = 1.32$ (s, 144H), 3.80 (s, 2H), 4.99 (s, 28H), 6.54–6.73 (m, 21H), 7.27 (d, $J = 1.6$ Hz, 16H), 7.39 (t, $J = 1.6$ Hz, 8H).

2.5. Synthesis of ***G_n-Perys***

To a quinoline suspension (5 ml) of 3,4:9,10-perylenetetracarboxylic dianhydride (50 mg, 0.125 mmol) were added **G_n-NH_2**, (0.3 mmol) and zinc acetate (17.5 mg, 0.08 mmol). The mixture was heated at 200 °C for 4 h under an argon atmosphere and, when the reaction was complete, the reaction mixture was poured into an aqueous solution (10 ml) of saturated

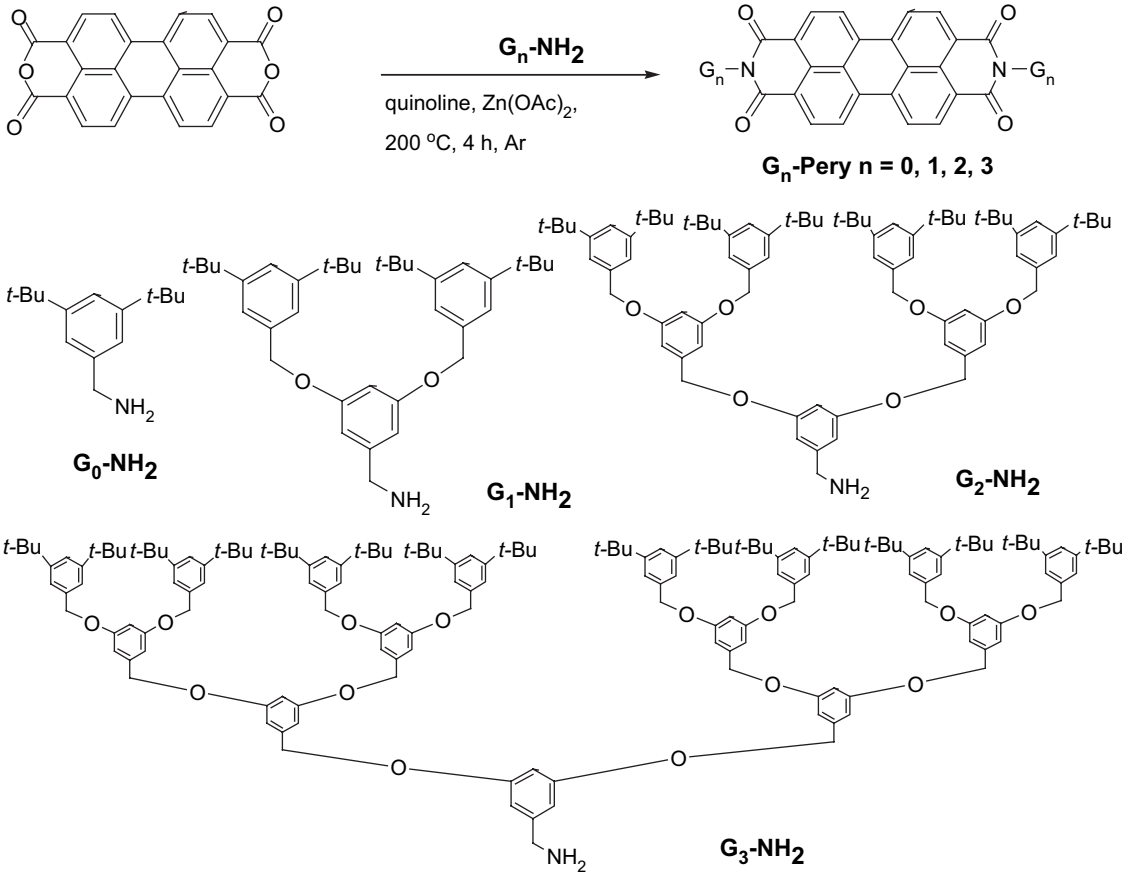

Scheme 1.

sodium hydrogen carbonate, followed by extraction with dichloromethane; the extract was dried over anhydrous sodium sulfate. **G_0-**, **G_1-**, and **G_2-Perys** were purified by column chromatography (SiO_2, dichloromethane). **G_3-Pery** was further purified by HPLC (column: Chromatorex-SI (Fuji-Davison Chemical Ltd.), pore size 70 Å, particle diameter 5 μm, 10 × 250 mm, developing solvent: hexane–isopropyl alcohol 98:2 mixed solvent (2 ml min^{-1}), detection: UV 254 nm).

2.5.1. *N,N′-Bis[-di(tert-butyl)benzyl]-3,4:9,10-perylenetetracarboxdiimide (**G_0-Pery**)*

Yield 80%; ^{1}H NMR ($CDCl_3$) $\delta = 1.32$ (s, 36H), 5.40 (s, 4H), 7.35 (t, $J = 1.1$ Hz, 2H), 7.49 (d, $J = 1.1$ Hz, 4H), 8.57 (d, $J = 8.0$ Hz, 4H), 8.68 (d, $J = 8.0$ Hz, 4H). Anal. Calcd for $C_{54}H_{54}N_2O_4$: C, 81.58; H, 6.85; N, 3.52%. Found: C, 81.89; H, 6.72; N, 3.38%.

2.5.2. *N,N′-Bis{3,5-bis[3,5-di(tert-butyl)benzyloxy]benzyl}-3,4:9,10-perylenetetracarboxdiimide (**G_1-Pery**)*

Yield 82%; ^{1}H NMR ($CDCl_3$) $\delta = 1.31$ (s, 72H), 4.97 (s, 8H), 5.39 (s, 4H), 6.60 (t, $J = 2.3$ Hz, 2H), 6.82 (d, $J = 2.3$ Hz, 4H), 7.25 (d, $J = 1.8$ Hz, 8H), 7.38 (t, $J = 1.8$ Hz, 4H), 8.63 (d, $J = 7.8$ Hz, 4H), 8.71 (d, $J = 7.8$ Hz, 4H). Anal. Calcd for $C_{98}H_{110}N_2O_8$: C, 81.52; H, 7.68; N, 1.94%. Found: C, 81.86; H, 7.63; N, 1.93%.

2.5.3. *N,N′-Bis(3,5-bis{3,5-bis[3,5-di(tert-butyl)benzyloxy]benzyloxy}benzyl)-3,4:9,10-perylenetetracarboxdiimide (**G_2-Pery**)*

Yield 81%; ^{1}H NMR ($CDCl_3$) $\delta = 1.32$ (s, 144H), 4.98 (s, 24H), 5.37 (s, 4H), 6.56 (t, $J = 1.8$ Hz, 2H), 6.61 (t, $J = 1.8$ Hz, 4H), 6.71 (d, $J = 1.8$ Hz, 8H), 6.82 (d, $J = 1.8$ Hz, 4H), 7.28 (d, $J = 1.5$ Hz, 16H), 7.39 (t, $J = 1.5$ Hz, 8H), 8.56 (d, $J = 8.1$ Hz, 4H), 8.69 (d, $J = 8.1$ Hz, 4H). Anal. Calcd for $C_{186}H_{222}N_2O_{16}$: C, 81.48; H, 8.16; N, 1.02%. Found: C, 81.08; H, 8.26; N, 0.89%.

2.5.4. *N,N′-Bis[3,5-bis(3,5-bis{3,5-bis[3,5-di(tert-butyl)benzyloxy]benzyloxy}-benzyloxy)benzyl]-3,4:9,10-perylenetetracarboxdiimide (**G_3-Pery**)*

Yield 88%; ^{1}H NMR ($CDCl_3$) $\delta = 1.31$ (s, 288H), 4.95–4.99 (m, 56H), 5.32 (br, 4H), 6.55–6.80 (m, 42H), 7.28 (d, $J = 1.8$ Hz, 32H), 7.39 (t, $J = 1.8$ Hz, 16H), 8.51–8.55 (m, 4H), 8.63–8.66 (m, 4H). Anal. Calcd for $C_{362}H_{446}N_2O_{32}$: C, 81.46; H, 8.42; N, 0.52%. Found: C, 81.76; H, 8.53; N 0.48%.

2.6. Solubility measurement

A saturated solution of **G_n-Perys** was prepared at 25 °C. The solution was filtered and diluted prior to UV–vis absorption measurement. The solubility was calculated on the basis of the known ε value at λ_{max} in the solvent.

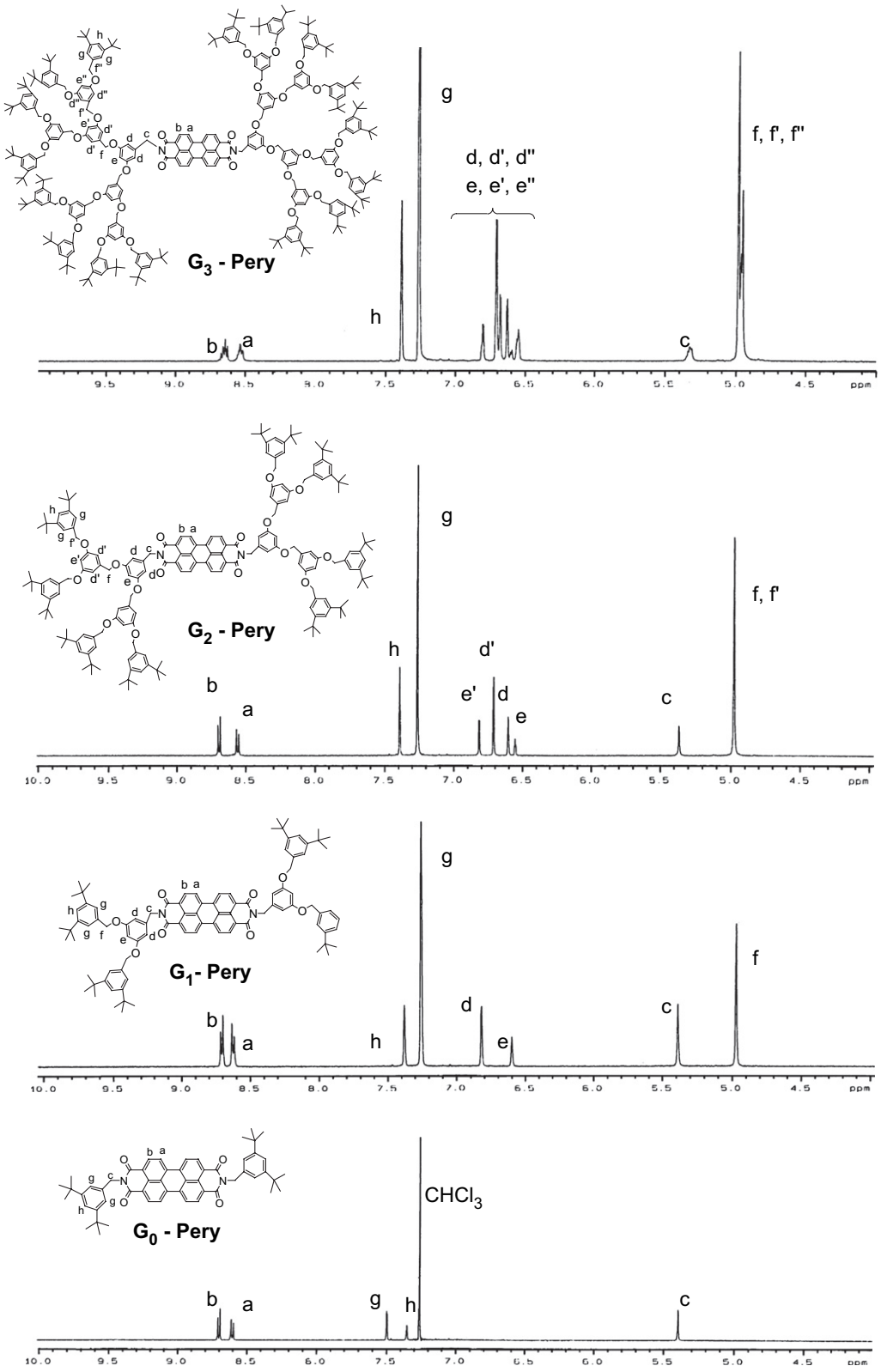

Fig. 2. ^{1}H NMR spectra of **G_n-Perys** in deuterochloroform.

2.7. Fabrication of EL device

ITO glass was sonicated in water, acetone, and isopropyl alcohol and the treated glass was kept in an ozone atmosphere under UV irradiation. The ITO glass was used as the anode. To a toluene solution (3 ml) of poly(vinylcarbazole) (PVK) (40 mg) and 2-(4-biphenyl)-5-(4-*tert*-butylphenyl)-1,3,4-oxaziazole (PBD) (40 mg) was added **G_n-Perys**. The ITO glass

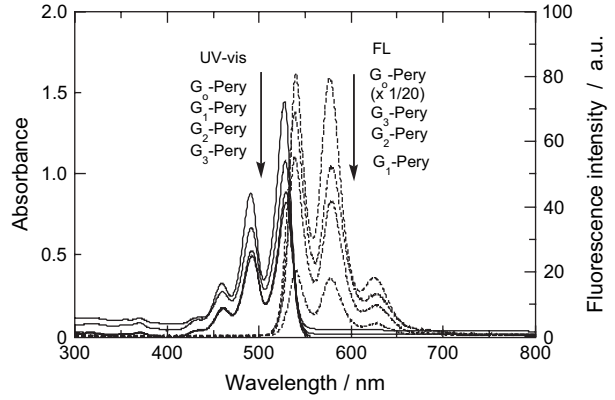

Fig. 3. UV–vis absorption and fluorescence spectra of **G_n-Perys** in chloroform at the concentration of 1×10^{-5} mol dm^{-3}.

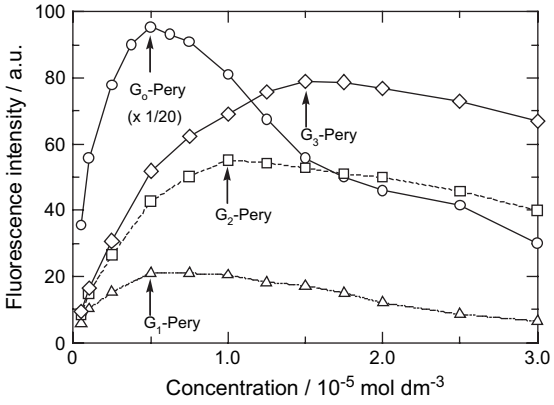

Fig. 4. Concentration-quenching of **G_n-Perys** in chloroform.

was spin-coated with the mixture (1000 rpm, 10 s then 2000 rpm, 10 s) and the film thickness was adjusted to 1000 Å. A cathode electrode of aluminum–lithium (99:1) alloy was prepared using a vapour deposition method (0.5 nm s^{-1}). The EL device and the chemical structures of PVK and PBD are shown in Fig. 1.

3. Results and discussion

3.1. Synthesis

G_n-Perys were synthesized by the reaction of perylene-3,4:9,10-tetracarboxylic dianhydride with amino dendrons **G_n-NH_2**, which were obtained by a Gabriel reaction of **G_n-Br**, in the presence of zinc acetate under an argon atmosphere in good yield as shown in Scheme 1.

Fig. 2 shows the ^{1}H NMR spectra of **G_n-Perys**. Two peaks at around 8.6 and 8.7 ppm were assigned to the aromatic protons **a** and **b** in the perylene nuclei, respectively. Doublet and triplet peaks at around 7.4 ppm were attributed to protons **g** and **h** in the peripheral aromatic rings, respectively. The proton peak **g** in **G_1-**, **G_2-**, and **G_3-Perys** upfielded and were observed at the same chemical shift of a chloroform proton. A series of triplet and doublet peaks belonging to the aromatic protons **d**, **d′**, **d″**, **e**, **e′**, and **e″** between the perylene and peripheral aromatic rings were observed in the range of 6.5–6.8 ppm. A singlet peak attributed to methylene protons **c** was observed at around 5.4 ppm. A series of singlet peaks assigned to the methylene protons **f**, **f′**, and **f″** were observed at around 5.0 ppm. A singlet peak of *t*-butyl protons was observed at 1.3 ppm.

3.2. UV–vis absorption and fluorescence spectra

Fig. 3 shows the UV–vis absorption and fluorescence spectra of **G_n-Perys** in chloroform. The characteristic three absorption maxima (λ_{max}) of **Pery** were observed at 460, 491, and 529 nm, there being no difference among **G_n-Perys**. Molar absorption coefficients (ε) at 529 nm were observed in the range of 74,700–144,600 dm^3 mol^{-1} cm^{-1}. Interestingly, the ε

Table 1
Physical properties of **G_n-Perys**

Compound	Mp/°C	λ_{max} (ε)[a]/nm	λ_{em}[b]/nm	Fluorescence intensity[b,c]	Solubility[d]/$\times 10^{-4}$ mol dm^{-3}		
					Hexane	Ether	Dichloromethane
G_0-Pery	>300	528 (144,600) 491 (87,300) 459 (31,800)	621 574 537	80	0.21	1.5	11
G_1-Pery	134–136	528 (107,600) 491 (66,200) 460 (26,600)	620 576 538	1.0	2.4	15	23
G_2-Prey	87–89	529 (85,800) 491 (50,400) 460 (15,600)	621 577 537	2.7	3.6	25	40
G_3-Prey	79–81	529 (74,700) 491 (44,200) 459 (9800)	621 576 537	3.4	4.2	31	48

[a] Measured in chloroform.
[b] Measured in chloroform at the concentration of 1×10^{-5} mol dm^{-3} at 25 °C (λ_{ex}: 528 nm).
[c] Arbitrary unit. Fluorescence intensity.
[d] Measured at 25 °C.

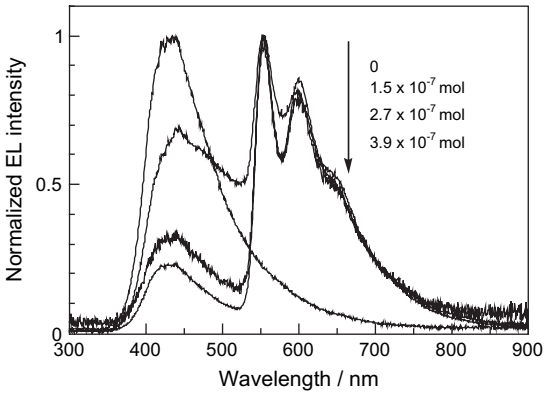

Fig. 5. EL spectra of **G_0-Perys**.

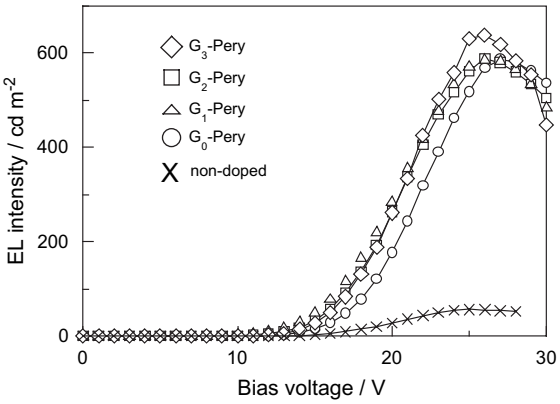

Fig. 7. Relationship between EL intensity and bias voltage.

value decreased at higher generation, which suggests twisting of the C–N bonds at the imido moieties in **G_n-Perys** due to the bulky dendrons. Photoluminescence (PL) maxima (λ_{em}) of **G_n-Perys** were observed at 537, 576, and 621 nm. These UV–vis absorption and fluorescence spectral data are listed in Table 1. The relative fluorescence intensities (RFI) of **G_1-**, **G_2-**, and **G_3-Perys** were ca. one-twentieth of that of **G_0-Pery** which can be attributed to either an increase in the internal conversion process or fluorescence quenching by the flexible 3,5-bis(benzyloxy) moieties. The fluorescence intensity of **G_0-Pery** in chloroform decreased to 98, 95, 81, and 73% in the presence of 2, 10, 20, and 100 molar amounts of **G_2-Br**, respectively. As 2 molar amounts of **G_2-Br** correspond to the amount of 3,5-bis(benzyloxy) moieties in **G_2-Pery**, the reduction in fluorescence intensity of **G_0-Pery** in the presence of **G_2-Br** was not remarkable. Thus, it is suggested that the increase in the internal conversion process by the flexible 3,5-bis(benzyloxy) moieties in **G_n-Perys** ($n = 1$, 2, 3) predominates.

The relationship between the concentration of **G_n-Perys** and fluorescence intensity is shown in Fig. 4. As the concentration of **G_n-Perys** increased the fluorescence intensity increased, reached a maximum point and decreased thereafter. The concentrations showing maximum fluorescence intensity were observed at 5×10^{-6}, 5×10^{-6}, 1×10^{-5}, and 1.5×10^{-5} mol dm^{-3} for **G_0-**, **G_1-**, **G_2-**, and **G_3-Pery**, respectively. As an example, the RFI at 2.0×10^{-5} mol dm^{-3} was in the following order: **G_3-Pery** > **G_2-Pery** > **G_1-Pery**. Thus, since fluorescence was also quenched by the intermolecular interactions operating between the perylene nuclei, at the same time, the bulky 3,5-bis(benzyloxy) dendrons can prevent these interactions so as to improve fluorescence intensity at higher generation.

3.3. Solubility

The solubilities of **G_n-Perys** in hexane, ether, and dichloromethane are indicated in Table 1. It is surprising that **Pery** is soluble in hexane. **G_n-Pery** was more soluble in the following order of solvent: dichloromethane > ether > hexane ≫ ethanol (<5×10^{-6} mol dm^{-3}). **G_n-Pery** was more soluble in all the solvents at higher generation. The melting point was lower at higher generation, indicating that the electrostatic intermolecular interactions between the imido moieties and/or π–π interactions between the perylene moieties were inhibited by introducing bulky dendrons.

3.4. Application of *G_n-Perys* as emitters in single-layer EL devices

The relationship between the amount of **G_0-Pery** and EL intensity is shown in Fig. 5. It has been reported that the EL

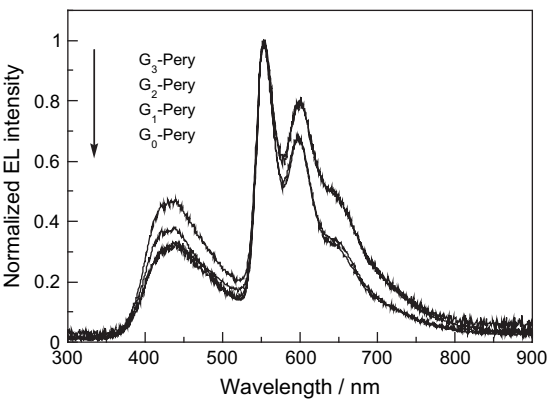

Fig. 6. EL spectra of **G_n-Perys** at the concentration of 2.7×10^{-7} mol.

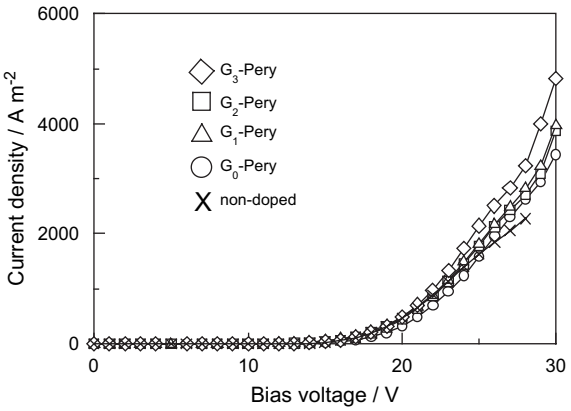

Fig. 8. Relationship between current density and bias voltage.

spectrum from PVK/PBD used as host molecules is observed at around 430 nm [9]. As the concentration of **G_0-Pery** increased, the EL peak at around 430 nm decreased slightly and that at around 600 nm increased slightly. The EL spectra of **G_n-Perys** were slightly bathochromic compared with the PL spectra in chloroform. When the concentration of **G_n-Perys** was 2.7×10^{-7} mol, white emission was observed due to EL peaks at 430 and 600 nm. The amount (1.5×10^{-7} mol) of **G_0-Pery** was sufficiently large compared with the other dopants. In our experience, when 1.5×10^{-7} mol of diazepines [10] and squarilium dendrimers [11] were doped in PVK/PBD, the emission band at 430 nm was scarcely observable. The emission at 430 nm in **G_n-Perys** was more intense than that of quinacridone dendrimers [11]. Thus, the energy-transfer form PVK/PBD to **G_0-Pery** does not smoothly proceed. Qu et al. have also reported that perylenetetracarboxidiimide having a polyphenylene dendron produced red emissions of low efficiency [7]. In our study of the properties of dye-centred dendrimers, the order of energy-transfer ability from PVK/PBD is roughly as follows: squariliums > quinacridones > perylenediimides.

Fig. 6 shows the EL spectra of **G_n-Perys** at a concentration of 2.7×10^{-7} mol; EL maxima were observed at around 430 and 600 nm. The emission at around 430 nm increased at higher generation, indicating that the energy-transfer from PVK/PBD to central **Pery** was inhibited by the bulky dendrons; a similar result has been reported for quinacridone-centred dendrimers [11].

Fig. 7 shows the relationship between EL intensity and bias voltage. While EL intensity increased by doping **G_n-Pery,** no remarkable difference in EL intensity under the fixed bias voltage was observed among **G_n-Perys**.

Fig. 8 shows the relationship between bias voltage and current density. Similar current density in the presence and in the absence of **G_n-Perys** was observed under the fixed bias voltage. No marked difference in the I–V characteristics was observed among **G_n-Perys**.

4. Conclusions

Novel **G_n-Perys** were synthesized by a convergent method in good yield. Absorption maxima, λ_{max}, of **G_n-Perys** were observed at 459, 491, and 529 nm in chloroform and λ_{em} were observed at 537, 576, and 621 nm. The fluorescence intensities of **G_1-**, **G_2-**, and **G_3-Perys** drastically decreased compared with that of **G_0-Pery**. Nevertheless, the concentration-quenching of **G_n-Pery** ($n = 1, 2, 3$) was improved at higher generation. **G_n-Perys** were more soluble in the following order of solvent: dichloromethane > ether > hexane ≫ ethanol; **G_n-Pery** was more soluble at higher generation. EL maxima of single-layer devices containing PVK, PBD, and **G_n-Pery** were observed at around 430 and 600 nm. No remarkable difference in the EL characteristics among **G_n-Perys** was observed. When the concentration of **G_0-Pery** was 2.7×10^{-7} mol, a white emission was observed.

References

[1] Jiang DL, Aida T. Photoisomerization in dendrimers by harvesting of low-energy photons. Nature 1997;388:454–6.

[2] Yokoyama S, Otomo A, Nakahama T, Mashiko S. Spiral photon confinement and super-radiation from dye cored dendrimer. Thin Solid Films 2001;393:124–8.

[3] Brewis M, Clarkson GJ, Goddard V, Heilliwell M, Holder AM, McKeown NB. Silicon phthalocyanines with axial dendritic substituents. Angew Chem Int Ed 1998;37:1092–4.

[4] Nakazawa T, Muto N, Mizuta Y, Kawahara A, Miyamoto E, Tsutsumi M, et al. A new type monolayered organic photoconductor for positive charging xerography. Chemistry and characteristics. Nippon Kagaku Kaishi:1007–18. Chem Abstr 1992;118:13833.

[5] Ferrere S, Gregg BA. New perylenes for dye sensitization of TiO_2. New J Chem 2002;26:1155–60.

[6] Ego C, Marsitzky D, Becker S, Zhang J, Grimsdale AC, Müllen K, et al. Attaching perylene dyes to polyfluorene: three simple, efficient methods for facile color tuning of light-emitting polymers. J Am Chem Soc 2003;125:437–43.

[7] Qu J, Zhang J, Grimsdale AC, Müllen K. Dendronized perylene diimide emitters: synthesis, luminescence, and electron and energy transfer studies. Macromolecule 2004;37:8297–306.

[8] Zeng F, Zimmerman SC, Kolotuchin SV, Reichert DEC, Ma Y. Supramolecular polymer chemistry: design, synthesis, characterization, and kinetics, thermodynamics, and fidelity of formation of self-assembled dendrimers. Tetrahedron 2002;58:825–43.

[9] Blumstengel S, Sokolik I, Dorsinville R, Voloschenko D, He M, Lavrentovich O, et al. Photo-, and electroluminescence studies of 2,5-bis[2′-4″-(6-hexoxybenzyl)-1′-ethenyl]-3,4-dibutyl thipphenes. Synth Met 1999;99:85–90.

[10] Horiguchi E, Kitaguchi T, Matsui M. Substituent effects of 6-substituted 3-dicyano-5-[4-(diethylamino)styryl]-7-methyl-6*H*-1,4-diazepines on the performance as red dopants in single-layer organic electroluminescence devices. Dyes Pigments 2006;70:43–7.

[11] Matsui M, Tanaka S, Funabiki K, Kitaguchi T. Synthesis, properties, and application as emitters in organic electroluminescence devices of quinacridone- and squarylium-dye-centred dendrimers. Bull Chem Soc Jpn 2006;79:170–6.